Appl Nanosci (2014) 4:753–760
DOI 10.1007/s13204-013-0255-4

ORIGINAL ARTICLE

A theoretical study of Prandtl nanofluid in a rectangular duct through peristaltic transport

Rahmat Ellahi · Arshad Riaz · S. Nadeem

Received: 11 June 2013 / Accepted: 2 July 2013 / Published online: 16 July 2013

Abstract In the current study, peristaltic transport of Prandtl nanofluid is investigated in a uniform rectangular duct. Interaction of peristaltic flow of non-Newtonian fluid model with nano particles is investigated under the long wave length and low Reynolds number approximations. The governing equations are solved by homotopy perturbation method to get the convergent series solution. Effects of all emerging physical parameters are demonstrated with the help of graphs for temperature distribution, nano particles concentration, pressure rise and pressure gradient. Trapping scheme is also described through streamlines.

Keywords Peristaltic transport · Prandtl fluid · Nano particles · Rectangular duct · Homotopy perturbation method (HPM)

Introduction

Peristalsis states a mechanism of pumping that is encountered in the case of most physiological fluids. Peristaltic transport appears in many physiological activities, including flow of urine from kidney to the bladder, in the movement of food material through the digestive tract, in flow of fluids through lymphatic vessels as well as in semen movement in the vas differences and spermatozoa inside the ductus efferentes of the male reproductive tract and cervical canal, in flow of ovum in the fallopian tube and also in the flow of blood through small blood vessels. This phenomenon is also applied in many biomedical equipments, such as finger pumps, heart-lung machine, blood pump machine and also in industries for the transport of noxious fluid in nuclear industries, as well as in roller pumps. In the view of such tremendous applications, studies of peristaltic movement have been receiving particular interest of scientific researchers like engineers, mathematicians and physicists etc. Due to the non linear variation of stress versus deformation rate in many applicable fluids, a number of researchers have been considering the studies of non-Newtonian fluids (Patel and Timol 2010; Ellahi et al. 2011; Ellahi and Zeeshan 2011; Mekheimer and Abdelmaboud 2008; Rafiq et al. 2010).

Many researchers have explored the studies of peristaltic flows with different types of Newtonian and non-Newtonian fluids (Tripathi et al. 2010; Tripathi 2011; Mekheimer et al. 2013; Kothandapani and Srinivas 2008) . Reddy et al. (2005) have analyzed the influence of lateral walls on peristaltic flow in a rectangular duct and concluded that the sagittal cross section of the uterus may be better approximated by a tube of rectangular cross section than a two-dimensional channel. Effect of lateral walls on peristaltic flow through an asymmetric rectangular duct has been recently investigated by Mekheimer et al. (2011).

Nanotechnology has emmence applications in industry since materials with sizes of nanometers exhibit unique physical and chemical properties. Fluids with nano-scaled

R. Ellahi · A. Riaz (✉)
Department of Mathematics and Statistics, FBAS, IIU, Islamabad 44000, Pakistan
e-mail: arshad.phdma03@iiu.edu.pk

R. Ellahi
e-mail: rellahi@engr.ucr.edu

S. Nadeem
Department of Mathematics, Quaid-i-Azam University, 45320, Islamabad 44000, Pakistan

R. Ellahi
Department of Mechanical Engineering, Bourns Hall A 373, University of California Riverside, Riverside, CA 92521, USA

particles interaction are called as nanofluid. The nano particles used in nanofluid are normally composed of metals, oxides, carbides or carbon nanotubes. Water, ethylene glycol and oil are common examples of base fluids. Nanofluid have their major applications in heat transfer, including microelectronics, fuel cells, pharmaceutical processes and hybrid-powered engines, domestic refrigerator, chiller, nuclear reactor coolant, grinding, space technology and in boiler flue gas temperature reduction. They demonstrate enhanced thermal conductivity and convective heat transfer coefficient counterbalanced to the base fluid. Nanofluid have been the core of attention of many researchers for new production of heat transfer fluids in heat exchangers, plants and automotive cooling significations, due to their enormous thermal characteristics (Nadeem et al. 2013). Under the enormous applications of nanofluids, the interaction of nano particles in peristaltic flows has now been receiving attentions of many researchers (Akbar and Nadeem 2012; Nadeem and Maraj 2012; Nadeem et al. 2013). To the best of author's information, study regrading the peristaltic flow of nanofluid with Prandtl model in a duct of three dimensional rectangular cross section has not been presented so far.

From the motivation of above discussion, authors decided to work on the peristaltic flow of Prandtl nanofluid in a uniform rectangular duct. The equations governing the flow are simplified under the assumptions of low Reynolds number and long wavelength. Then the non dimensionalized and non linear partial differential equations are solved through homotopy perturbation method (HPM). The pertinent physical parameters affecting the flow are analyzed graphically. Temperature, nano particles concentration, pressure gradient and pressure rise plots are explained with the variation of various quantities. Trapping bolus scheme is also elaborated through streamlines examining the flow pattern of the considered problem.

Mathematical model

Let us analyze the peristaltic flow of a Prandtl fluid with nano particles concentration in a cross section of three dimensional uniform rectangular channel. The flow is initiated by the propagation of sinusoidal waves having wave length λ travelling along the axial direction of the channel with constant speed c. The constitutive relations for Prandtl fluid are described with the help of a general expression ($\boldsymbol{\tau}$) as defined below (Patel and Timol 2010)

$$\boldsymbol{\tau} = \frac{A \sin^{-1}\left(\frac{1}{C}\left(\left(\frac{\partial U}{\partial Y}\right)^2+\left(\frac{\partial W}{\partial Y}\right)^2\right)^{1/2}\right)}{\left(\left(\frac{\partial U}{\partial y}\right)^2+\left(\frac{\partial W}{\partial y}\right)^2\right)^{1/2}}\frac{\partial U}{\partial Y}, \tag{1}$$

in which A and C represent material constants of Prandtl fluid model. The peristaltic waves on the walls are represented as (Nadeem and Maraj 2012)

$$Z = \pm H(X,t) = \pm a \pm b\cos\left[\frac{2\pi}{\lambda}(X-ct)\right],$$

where a and b are the amplitudes of the waves, t is the time, and X is the direction of wave propagation.

Formulation of the problem

Let us define a wave frame (x, y) moving with the velocity c away from the fixed frame (X, Y) by the following transformation

$$x = X - ct, \quad y = Y, \quad z = Z, \quad u = U - c,$$
$$w = W, \quad p(x,y,z) = P(X,Y,Z,t). \tag{2}$$

The walls parallel to XZ-plane remain undisturbed and are not subject to any peristaltic wave motion. We assume that the lateral velocity is zero as there is no change in lateral direction of the duct cross section. To reduce the number of extra parameters, we define the following non-dimensional quantities

$$\bar{x} = \frac{x}{\lambda}, \quad \bar{y} = \frac{y}{d}, \quad \bar{z} = \frac{z}{a}, \quad \bar{t} = \frac{c}{\lambda}t, \quad \bar{u} = \frac{u}{c}, \quad \bar{w} = \frac{w}{c\delta},$$
$$\theta = \frac{T-T_0}{T_1-T_0}, \quad \sigma = \frac{C-C_0}{C_1-C_0}, \quad \bar{h} = \frac{H}{a},$$
$$\delta = \frac{a}{\lambda}, \quad \phi = \frac{b}{a}, \quad B_r = \frac{\rho_f g \alpha_f a^2}{\mu c}(C_1 - C_0),$$
$$G_r = \frac{\rho_f g \alpha_f a^2}{\mu c}(T_1 - T_0), \quad \alpha_f = \frac{K}{(\rho c)_f},$$
$$N_b = \frac{\tau D_B}{\alpha_f}(C_1 - C_0), \quad N_t = \frac{D_T}{T_0 \alpha_f}(T_1 - T_0),$$
$$S_c = \frac{\mu}{\rho D_B}, \quad P_r = \frac{\mu}{\rho \alpha_f}, \quad \bar{\boldsymbol{\tau}} = \frac{a}{\mu c}\boldsymbol{\tau}, \quad \beta = \frac{a}{d}, \quad \bar{p} = \frac{a^2 p}{\mu c \lambda},$$
$$\alpha = \frac{A}{\mu C}, \quad \beta_1 = \frac{\alpha c^2}{6C^2 a^2}, \quad \tau = (\rho c)_p/(\rho c)_f, \quad Re = \frac{\rho a c}{\mu}.$$

Therefore, the non-dimensional governing equations (after exempting the bar symbols) for Prandtl nano fluid in a wave frame with velocity field $(u, 0, w)$ will obtain the following expressions

$$\frac{\partial u}{\partial x} + \frac{\partial w}{\partial z} = 0, \tag{3}$$

$$Re\delta\left(u\frac{\partial u}{\partial x} + w\frac{\partial u}{\partial z}\right) = -\frac{\partial p}{\partial x} + \delta\frac{\partial}{\partial x}\tau_{xx} + \beta^2\frac{\partial}{\partial y}\tau_{xy} + \frac{\partial}{\partial z}\tau_{xz}, \tag{4}$$

$$0 = -\frac{\partial p}{\partial y} + \delta^2\frac{\partial}{\partial x}\tau_{yx} + \delta^2\frac{\partial}{\partial y}\tau_{yy} + \delta\frac{\partial}{\partial z}\tau_{yz}, \tag{5}$$

$$Re\delta^2\left(u\frac{\partial w}{\partial x}+w\frac{\partial w}{\partial z}\right)=-\frac{\partial p}{\partial z}+\delta^2\frac{\partial}{\partial x}\tau_{zx}+\delta\beta^2\frac{\partial}{\partial y}\tau_{zy}+\delta^2\frac{\partial}{\partial z}\tau_{zz}. \quad (6)$$

$$Re\delta P_r\left(u\frac{\partial \theta}{\partial x}+w\frac{\partial \theta}{\partial z}\right)=\delta^2\frac{\partial^2\theta}{\partial x^2}+\beta^2\frac{\partial^2\theta}{\partial y^2}+\frac{\partial^2\theta}{\partial z^2}+N_b\left(\delta^2\frac{\partial\theta}{\partial x}\frac{\partial\sigma}{\partial x}+\beta^2\frac{\partial\theta}{\partial y}\frac{\partial\sigma}{\partial y}+\frac{\partial\theta}{\partial z}\frac{\partial\sigma}{\partial z}\right)+N_t\left(\delta^2\left(\frac{\partial\theta}{\partial x}\right)^2+\beta^2\left(\frac{\partial\theta}{\partial y}\right)^2+\left(\frac{\partial\theta}{\partial z}\right)^2\right), \quad (7)$$

$$Re\delta S_c\left(u\frac{\partial \sigma}{\partial x}+w\frac{\partial \sigma}{\partial z}\right)=\delta^2\frac{\partial^2\sigma}{\partial x^2}+\beta^2\frac{\partial^2\sigma}{\partial y^2}+\frac{\partial^2\sigma}{\partial z^2}+\frac{N_t}{N_b}\left(\delta^2\frac{\partial^2\theta}{\partial x^2}+\beta^2\frac{\partial^2\theta}{\partial y^2}+\frac{\partial^2\theta}{\partial z^2}\right), \quad (8)$$

where P_r, N_b, N_t, G_r, B_r, α and β_1 demonstrate the Prandtl number, the Brownian motion parameter, the thermophoresis parameter, local temperature Grashof number, local nano particle Grashof number and the dimensionless parameters of Prandtl fluid, respectively. The boundaries of the channel will obtain the dimensionless form as follows

$$z=\pm h(x)=\pm 1\pm\phi\cos 2\pi x. \quad (9)$$

Under the assumptions of long wave length $\delta \leq 1$ and low Reynolds number $Re \longrightarrow 0$ (see Nadeem et al. 2013) Eq. (3) is identically satisfied and Eqs. (4)–(8) simplify to the following form

$$\frac{1}{\alpha}\frac{dp}{dx}=\beta^2\frac{\partial^2 u}{\partial y^2}+\frac{\partial^2 u}{\partial z^2}+\frac{3\beta_1}{\alpha}\left(\beta^4\left(\frac{\partial u}{\partial y}\right)^2\frac{\partial^2 u}{\partial y^2}+\left(\frac{\partial u}{\partial z}\right)^2\frac{\partial^2 u}{\partial z^2}\right)+\frac{1}{\alpha}(B_r\sigma+G_r\theta), \quad (10)$$

$$\beta^2\frac{\partial^2\theta}{\partial y^2}+\frac{\partial^2\theta}{\partial z^2}+N_b\left(\beta^2\frac{\partial\theta}{\partial y}\frac{\partial\sigma}{\partial y}+\frac{\partial\theta}{\partial z}\frac{\partial\sigma}{\partial z}\right)+N_t\left(\beta^2\left(\frac{\partial\theta}{\partial y}\right)^2+\left(\frac{\partial\theta}{\partial z}\right)^2\right)=0, \quad (11)$$

$$\beta^2\frac{\partial^2\sigma}{\partial y^2}+\frac{\partial^2\sigma}{\partial z^2}+\frac{N_t}{N_b}\left(\beta^2\frac{\partial^2\theta}{\partial y^2}+\frac{\partial^2\theta}{\partial z^2}\right)=0. \quad (12)$$

The corresponding boundary conditions are

$$u=-1 \text{ at } y=\pm 1, \quad u=-1 \text{ at } z=\pm h(x), \quad (13)$$

$$\theta=0 \text{ at } z=h(x), \quad \theta=1 \text{ at } z=-h(x), \quad (14)$$

$$\sigma=0 \text{ at } z=h(x), \quad \sigma=1 \text{ at } z=-h(x). \quad (15)$$

The expressions for the non-dimensional stream functions can be described as $u=\partial\psi/\partial z$, $w=-\partial\psi/\partial y$, where ψ represents the stream function.

Solution of the problem

Solution by homotopy perturbation method

The solution of the above nonlinear partial differential equations $(10-12)$ have been calculated by homotopy perturbation method (HPM). The homotopy for considered problems are constructed as (He 2006, 2010; Saadatmandi et al. 2009)

$$H(v,q)=(1-q)£[v-\widetilde{v}_0]+q\left(£[v]+\beta^2\frac{\partial^2 v}{\partial y^2}+\frac{3\beta_1}{\alpha}\left(\beta^4\left(\frac{\partial v}{\partial y}\right)^2\frac{\partial^2 v}{\partial y^2}+\left(\frac{\partial v}{\partial z}\right)^2\frac{\partial^2 v}{\partial z^2}\right)+\frac{1}{\alpha}\left(B_r\Omega+G_r\Theta-\frac{dp}{dx}\right)\right)=0, \quad (16)$$

$$H(\Theta,q)=(1-q)£\left[\Theta-\widetilde{\theta}_0\right]+q\left(£[\Theta]+\beta^2\frac{\partial^2\Theta}{\partial y^2}+N_b\left(\beta^2\frac{\partial\Omega}{\partial y}\frac{\partial\Theta}{\partial y}+\frac{\partial\Omega}{\partial z}\frac{\partial\Theta}{\partial z}\right)+N_t\left(\beta^2\left(\frac{\partial\Theta}{\partial y}\right)^2+\left(\frac{\partial\Theta}{\partial z}\right)^2\right)\right)=0, \quad (17)$$

$$H(\Omega,q)=(1-q)£[\Omega-\widetilde{\sigma}_0]+q\left(£[\Omega]+\beta^2\frac{\partial^2\Omega}{\partial y^2}+\frac{N_t}{N_b}\left(\beta^2\frac{\partial^2\Theta}{\partial y^2}+\frac{\partial^2\Theta}{\partial z^2}\right)\right)=0. \quad (18)$$

Here, £ gives the linear operator chosen as $£=\partial^2/\partial z^2$. Let the initial solutions are as follow

$$\widetilde{v}_0=-1+\left(z^2-h^2\right)+\frac{1}{\beta^2}\left(1-y^2\right), \quad (19)$$

$$\widetilde{\theta}_0=\beta^2\left(z^2-h^2\right)+\frac{h-z}{2h}=\widetilde{\sigma}_0. \quad (20)$$

Let us define

$$v(x,y,z)=v_0+qv_1+q^2v_2+\ldots$$
$$\Theta(x,y,z)=\Theta_0+q\Theta_1+q^2\Theta_2+\ldots \quad (21)$$
$$\Omega(x,y,z)=\Omega_0+q\Omega_1+q^2\Omega_2+\ldots$$

Incorporating Eq. (21) into Eqs. (16)–(18) and then equating the powers of q, one observes the system of equations along with the relative boundary conditions. According to the scheme of the HPM, we have the final solutions as $q \longrightarrow 1$ and are defined as

$$u(x,y,z)=v(x,y,z)|_{q\to 1}=v_0+v_1+v_2+\ldots$$
$$\theta(x,y,z)=\Theta(x,y,z)|_{q\to 1}=\Theta_0+\Theta_1+\Theta_2+\ldots \quad (22)$$
$$\sigma(x,y,z)=\Omega(x,y,z)|_{q\to 1}=\Omega_0+\Omega_1+\Omega_2+\ldots$$

The resulting series solutions for velocity, temperature and nano particles concentration are evaluated by using Eq. (22) as (when $q \longrightarrow 1$) and are discovered as

$$u(x,y,z) = \frac{1}{1440h^2N_b\alpha^2\beta^2}\big(15G_rN_b(N_b+N_t)z^4\alpha\beta^2 + 8h^5N_bz\beta^2\big(-7G_r(N_b+N_t)\alpha\beta^2+48(B_r+G_r)\beta_1\big)$$
$$+24hN_bz^3\beta^2\big(5(B_r+G_r)\alpha - G_r(N_b+N_t)z^2\alpha\beta^2 - 36(B_r+G_r)z^2\beta_1\big)$$
$$+40h^3N_bz\beta^2\big(-3(B_r+G_r)\alpha+2G_r(N_b+N_t)z^2\alpha\beta^2+12(B_r+G_r)z^2\beta_1\big) + 32h^8N_b\beta^2\big(7G_r(N_b+N_t)\alpha\beta^4$$
$$+105(B_r+G_r)\beta^2\beta_1 - 720\beta_1^2\big) + 120h^6\big(-5((B_r+G_r)N_b - B_rN_t)\alpha\beta^4 - 2G_rN_b(N_b+N_t)z^2\alpha\beta^6$$
$$-6N_b\big(3(B_r+G_r-2p)\beta^2+4\alpha(-3+\beta^2)\big)\beta_1 - 3456N_by^2\beta_1^2\big) + 15h^4(\alpha(-96N_b\alpha$$
$$+N_b(24B_r+G_r(24+5N_b+5N_t) - 48(\mathrm{d}p/\mathrm{d}x+4\alpha))\beta^2 + 48((B_r+G_r)N_b - B_rN_t)z^2\beta^4\big)$$
$$-288N_b\big(4y^2\alpha - 4z^2\alpha\beta^2 + (B_r+G_r)z^4\beta^4\big)\beta_1 + 41472N_by^2z^2\beta_1^2\big) + 2h^2\big(\alpha\big(-720N_b\big(-1+y^2-z^2\big)\alpha$$
$$-45N_b\big(16\alpha+z^2(4B_r+G_r(4+N_b+N_t) - 8(\mathrm{d}p/\mathrm{d}x+4\alpha))\big)\beta^2 - 60((B_r+G_r)N_b - B_rN_t)z^4\beta^4$$
$$+8G_rN_b(N_b+N_t)z^6\beta^6\big) + 120N_bz^2\big(72y^2\alpha + z^2(9(B_r+G_r-2\mathrm{d}p/\mathrm{d}x)\beta^2 + 4(B_r+G_r)z^2\beta^4$$
$$-12\alpha(3+5\beta^2)\big)\big)\beta_1 + 11520N_bz^4\big(-9y^2+z^2\beta^2\big)\beta_1^2\big)\big), \tag{23}$$

$$\theta(x,y,z) = \frac{1}{720h^3}\big(-15\big(N_b^2+3N_bN_t+2N_t^2\big)z^3 - 720h^5\beta^2 + 240h^7N_b\beta^4 + 16h^6\big(N_b^2+3N_bN_t+2N_t^2\big)z\beta^4$$
$$-64h^9\big(N_b^2+3N_bN_t+2N_t^2\big)\beta^6 + 40h^4z\beta^2\big(2N_b^2z^2\beta^2 + 6N_b\big(-1+N_tz^2\beta^2\big) + N_t\big(-3+4N_tz^2\beta^2\big)\big)$$
$$+30hz^2\big(2N_b^2z^2\beta^2 + N_t\big(-3+4N_tz^2\beta^2\big) + N_b\big(-3+6N_tz^2\beta^2\big)\big) + 2h^3(180+45N_t+360z^2\beta^2 - 60N_t^2z^2\beta^2$$
$$+64N_t^2z^6\beta^6 + N_b^2\big(-30z^2\beta^2+32z^6\beta^6\big) + 3N_b\big(15-30N_tz^2\beta^2 - 40z^4\beta^4 + 32N_tz^6\beta^6\big)\big)$$
$$-3h^2z\big(N_b^2\big(-5+32z^4\beta^4\big) + N_b\big(-80z^2\beta^2+3N_t\big(-5+32z^4\beta^4\big)\big) + 2\big(60-20N_tz^2\beta^2+N_t^2\big(-5+32z^4\beta^4\big)\big)\big)\big), \tag{24}$$

$$\sigma(x,y,z) = \frac{h-z}{2h} + \big(-h^2+z^2\big)\beta^2 + \frac{h^2N_t\beta^2 - N_tz^2\beta^2}{N_b} + \frac{1}{24h^2N_b}\big(-3h^2N_bN_t - 3h^2N_t^2 + 3N_bN_tz^2 + 3N_t^2z^2 + 8h^3N_bN_tz\beta^2$$
$$+8h^3N_t^2z\beta^2 - 8hN_bN_tz^3\beta^2 - 8hN_t^2z^3\beta^2 - 8h^6N_bN_t\beta^4 - 8h^6N_t^2\beta^4 + 8h^2N_bN_tz^4\beta^4 + 8h^2N_t^2z^4\beta^4\big). \tag{25}$$

The average volume flow rate over one period $\left(T = \frac{\lambda}{c}\right)$ of the peristaltic wave is defined as

$$Q = \int_0^{h(x)}\int_0^1 (u(x,y,z)+1)\mathrm{d}y\mathrm{d}z. \tag{26}$$

The pressure gradient $\mathrm{d}p/\mathrm{d}x$ is obtained from the expression of flow rate and is described as

$$\frac{\mathrm{d}p}{\mathrm{d}x} = \big(-3360hN_b\alpha^2 + 5040N_bQ\alpha^2\beta^2$$
$$-21h^3N_b\alpha((35B_r+G_r(35+8N_b+8N_t))\beta^2$$
$$-160\alpha\big(1+2\beta^2\big) - 640\beta_1\big)$$
$$-512h^7N_b\beta^2\big(G_r(N_b+N_t)\alpha\beta^4 + 18(B_r+G_r)\beta^2\beta_1$$
$$-135\beta_1^2\big) + 42h^5((32B_r(N_b-N_t)$$
$$+G_rN_b(32+N_b+N_t)).\alpha\beta^4 + 2N_b$$
$$\big(-288\alpha + 65(B_r+G_r)\beta^2\big)\beta_1 + 6912N_b\beta_1^2\big)\big)$$
$$/\big(336h^3N_b\beta^2\big(-5\alpha+36h^2\beta_1\big)\big). \tag{27}$$

The pressure rise Δp is evaluated by numerically integrating the pressure gradient $\mathrm{d}p/\mathrm{d}x$ over one wavelength, i.e.,

$$\Delta p = \int_0^1 \frac{\mathrm{d}p}{\mathrm{d}x}\mathrm{d}x. \tag{28}$$

Results and discussions

In the present section of the study, we demonstrate the physical and graphical variation of the results obtained above with different physical parameters affecting the flow phenomenon and the discussion on the part of graphical treatment may lead to various physical and industrial applications for many disciplines under different situations. The graphs for temperature profile are described through Figs. 1 and 2, nano particles concentration through Figs. 3 and 4, pressure rise through Figs. 5, 6, 7, 8 and pressure gradient through Figs. 9, 10, 11. The trapping bolus phenomenon is also explained through Figs. 12, 13, 14.

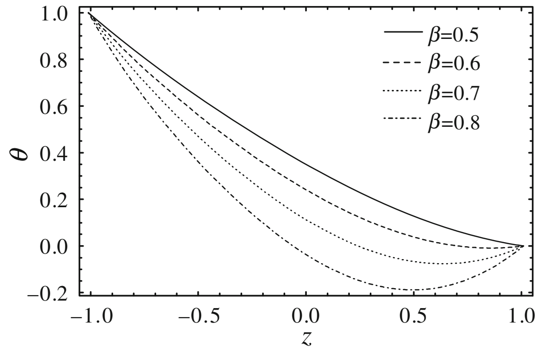

Fig. 1 Temperature profile θ for different values of β for fixed $N_t = 0.5$, $N_b = 0.3$, $\phi = 0.01$, $x = 0$, $y = 1$

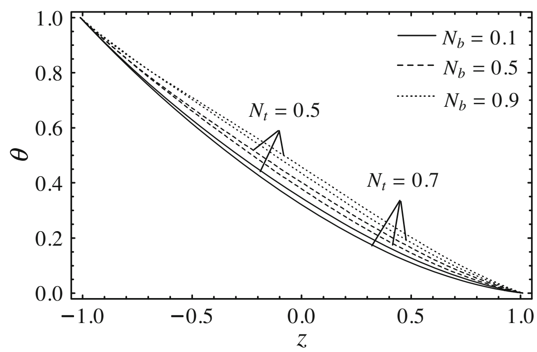

Fig. 2 Temperature profile θ for different values of N_b and N_t for fixed $\beta = 0.5$, $\phi = 0.01$, $x = 0$, $y = 1$

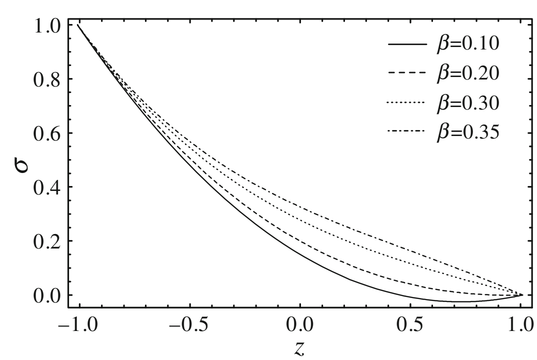

Fig. 3 Nano particles concentration profile σ for different values of β for fixed $N_t = 0.8$, $N_b = 0.3$, $\phi = 0.01$, $x = 0$, $y = 1$

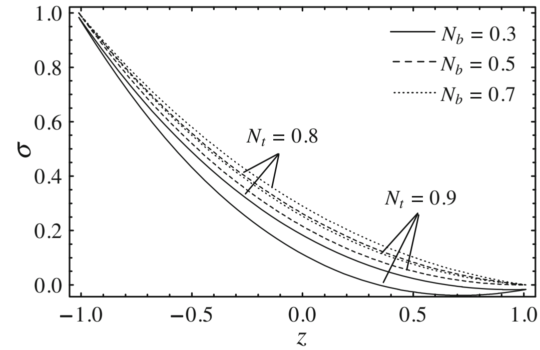

Fig. 4 Nano particles concentration profile σ for different values of N_b and N_t for fixed $\beta = 0.2$, $\phi = 0.01$, $x = 0$, $y = 1$

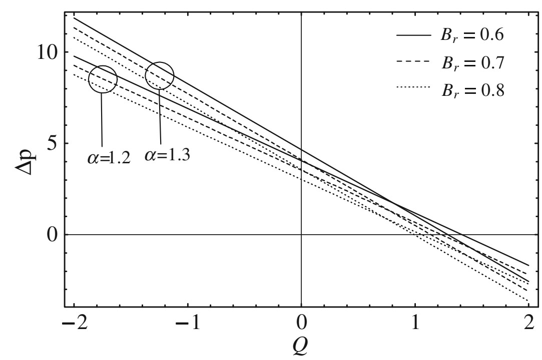

Fig. 5 Variation of pressure rise Δp with α and B_r at $N_t = 0.7$, $N_b = 0.6$, $G_r = 0.6$, $\beta = 2.1$, $\beta_1 = 0.5$, $\phi = 0.2$

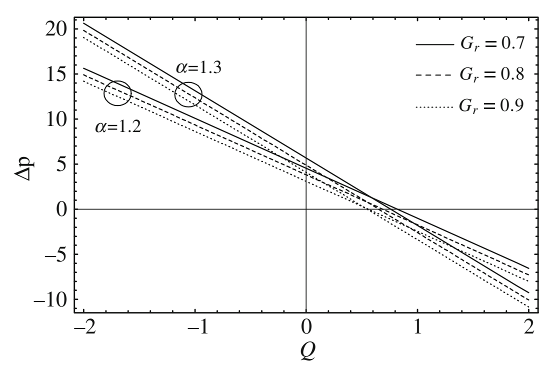

Fig. 6 Variation of pressure rise Δp with G_r and α at $N_t = 0.7$, $N_b = 0.6$, $B_r = 0.6$, $\phi = 0.3$, $\beta = 2.1$, $\beta_1 = 0.5$

Figure 1 contains the variation of temperature profile θ along axial direction while varying the values of aspect ratio β (lateral walls parameter) and it is measured here that the increase in β (either by increasing height a or by decreasing width d of the channel) suppresses the profile of temperature i.e., heat of the flow reduces with changing lateral walls. From Fig. 2, one can observe that temperature profile θ increases with an increase in the Brownian motion parameter N_b but decreases with the thermophoresis parameter N_t. It is noticed from Fig. 3 that increasing lateral walls dimensions increases the nano particles concentration σ . The effects of N_b and N_t on nano particles phenomenon σ can be observed from Fig. 4. It is to be noted here that the similar variation appears for σ against N_b and N_t as that of seen for θ .

Figure 5 gives the variation of pressure rise Δp against the flow rate axis Q with Prandtl parameter α and local nano particle Grashof number B_r. We can see that in peristaltic pumping $(\Delta p > 0, Q > 0)$ and retrograde pumping region $(\Delta p > 0, Q < 0)$, the pressure rise curves

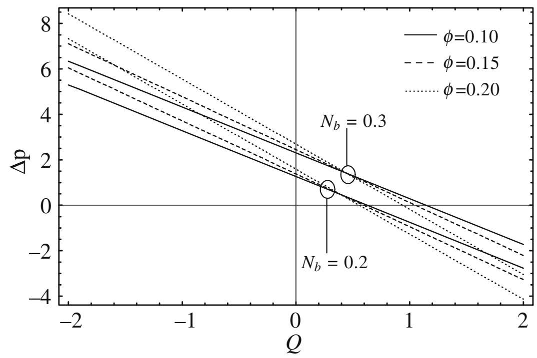

Fig. 7 Variation of pressure rise Δp with N_b and ϕ at $N_t = 0.7$, $G_r = 0.7$, $B_r = 0.6$, $\alpha = 1.2$, $\beta = 2.1$, $\beta_1 = 0.5$

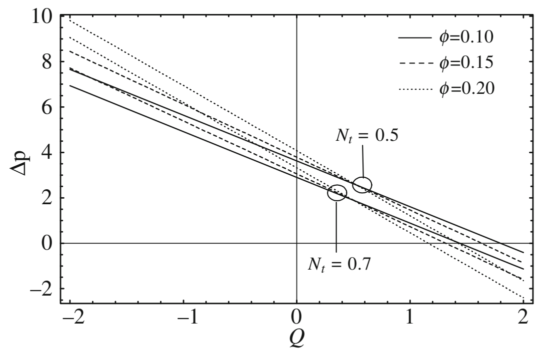

Fig. 8 Variation of pressure rise Δp with N_t and ϕ at $N_b = 0.7$, $G_r = 0.7$, $B_r = 0.6$, $\alpha = 1.2$, $\beta = 2.1$, $\beta_1 = 0.5$

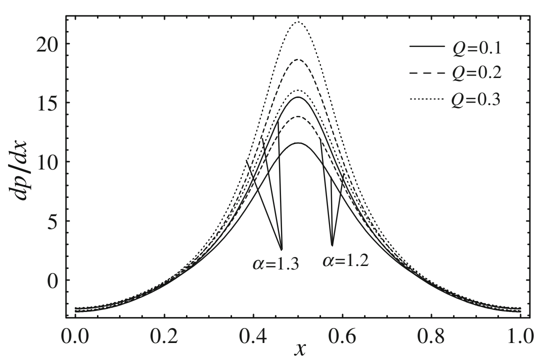

Fig. 9 Variation of pressure gradient dp/dx with α and Q at $N_t = 0.5$, $N_b = 0.1$, $G_r = 0.9$, $\beta_1 = 0.5$, $\phi = 0.3$, $B_r = 0.8$, $\beta = 1.9$

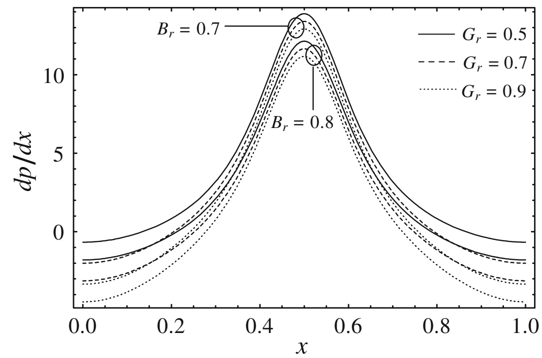

Fig. 10 Variation of pressure gradient dp/dx with B_r and G_r at $N_t = 0.5$, $N_b = 0.1$, $\alpha = 1.2$, $\beta_1 = 0.5$, $\phi = 0.3$, $Q = 0.2$, $\beta = 2$

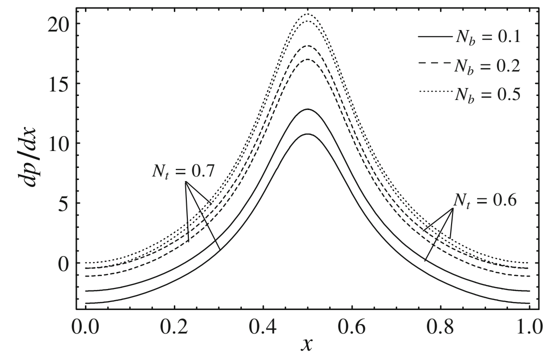

Fig. 11 Variation of pressure gradient dp/dx with N_b and N_t at $\alpha = 1.2$, $Q = 0.2$, $G_r = 0.7$, $\beta_1 = 0.5$, $\phi = 0.3$, $B_r = 0.5$, $\beta = 2.1$

decreases with B_r and increases with α and opposite results are shown in the copumping part i.e., $(\Delta p < 0, Q > 0)$. It is also clear that free pumping $(\Delta p = 0)$ occurs at $Q = 0.3$. Figure 6 reveals the similar effects for Δp under the variation of α and local temperature Grashof number G_r. It is depicted from Fig. 7 that peristaltic pumping rate increases with N_b and ϕ in peristaltic pumping and retrograde pumping parts while reversed in the copumping area but opposite behavior is observed for N_t as shown in Fig. 8.

Figure 9 implies the variation of pressure gradient curves dp/dx with α and flow rate Q drawn along the x-axis. It can be explained from this figure that dp/dx is an increasing function of both the parameters, also in the central part of the plane, pressure gradient gets maximum change as compared with the boundary walls. It admits that in the centre of the x-region, much pressure is required to make the flow consistent as compared with the corner regions. It can be extracted from Fig. 10 that pressure gradient profile is inversely varying with G_r and B_r and maximum change in pressure occurs at $x = 0.5$. From Fig. 11, it is concluded that dp/dx is increasing with N_b and decreasing with N_t but remains uniform throughout the domain.

Trapping bolus scheme for the local temperature Grashof number G_r can be observed from Fig. 12 and one comes to know that the circulating central bolus is decreased in size but enclosed by more streamlines as we increase the value of G_r. However, there is a quite opposite story for prandtl parameter α i.e., by increasing the value of α, size of the bolus starts increasing but numbers of bolus becomes two at $\alpha = 1.5$ which was three at the initial value of α i.e., $\alpha = 1.3$ (see Fig. 13). Figure 14 discloses that the

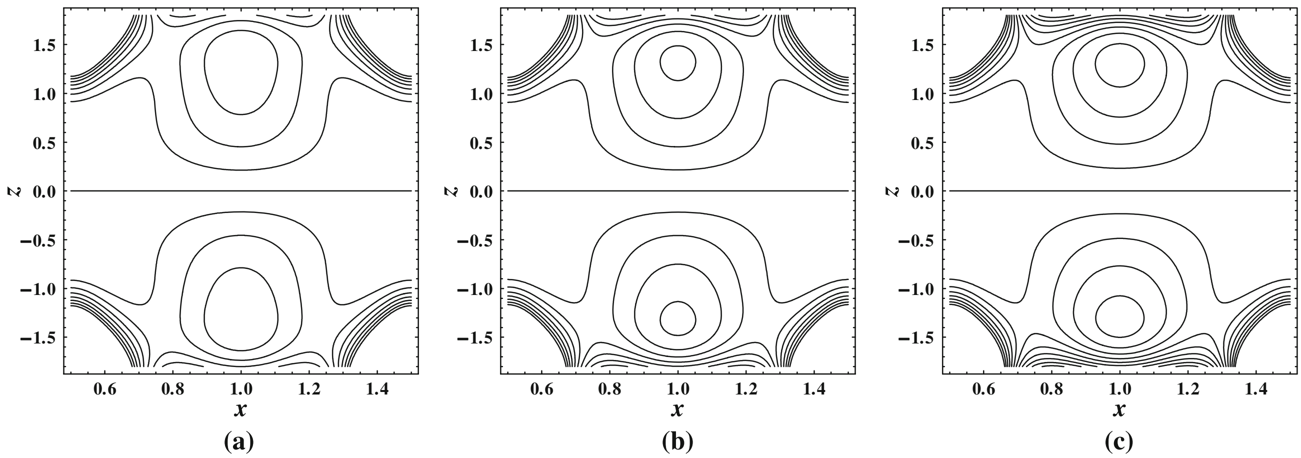

Fig. 12 Stream lines for different values of G_r, **a** for $G_r = 0.5$, **b** for $G_r = 0.7$, **c** for $G_r = 0.9$. The other parameters are $B_r = 0.8$, $\beta = 2.6$, $N_t = 0.5$, $\alpha = 1.5$, $N_b = 0.5$, $\phi = 0.3$, $Q = 1$, $y = 1$, $\beta_1 = 0.5$

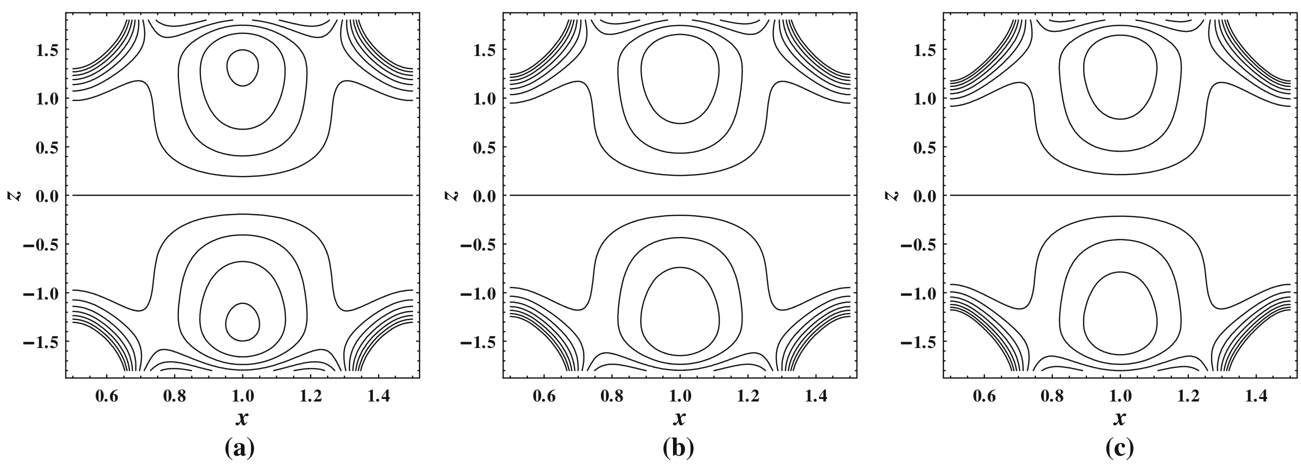

Fig. 13 Stream lines for different values of α, **a** for $\alpha = 1.3$, **b** for $\alpha = 1.4$, **c** for $\alpha = 1.5$. The other parameters are $B_r = 0.8$, $\beta = 2.6$, $N_t = 0.5$, $G_r = 0.5$, $N_b = 0.5$, $\phi = 0.3$, $Q = 1$, $y = 1$, $\beta_1 = 0.5$

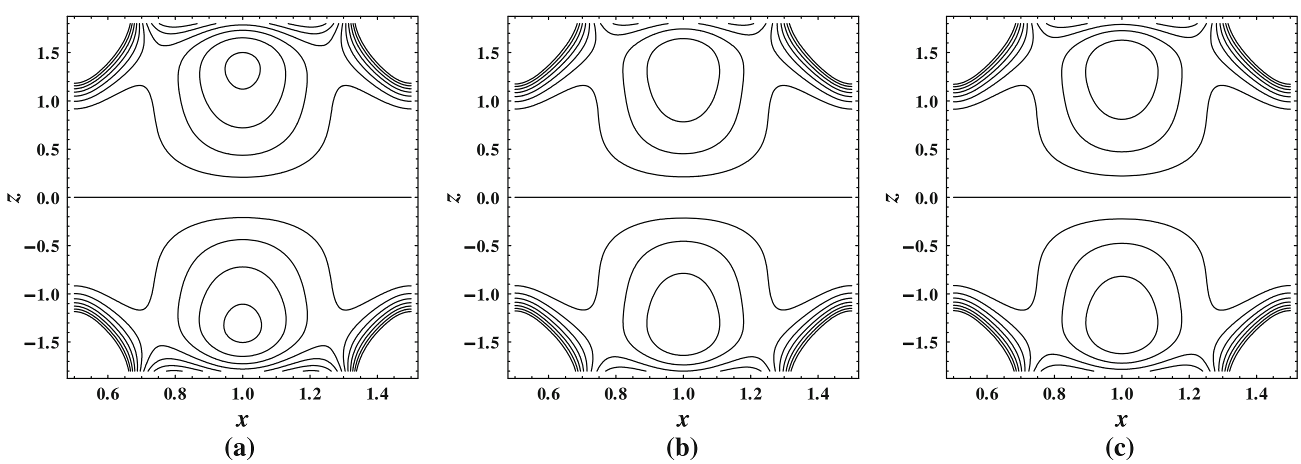

Fig. 14 Stream lines for different values of N_b, **a** for $N_b = 0.2$, **b** for $N_b = 0.5$, **c** for $N_b = 0.8$. The other parameters are $B_r = 0.8$, $\beta = 2.6$, $N_t = 0.5$, $\alpha = 1.5$, $G_r = 0.5$, $\phi = 0.3$, $Q = 1$, $y = 1$, $\beta_1 = 0.5$

behavior of circulating bolus is quite similar for the Brownian motion parameter N_b as that was seen for G_r.

Outcomes of the study

In the present analysis, we have tried to discover the theoretical investigation of the peristaltic phenomenon for Prandtl nano fluid in a three dimensional rectangular duct. We have employed homotopy perturbation method to deal with highly nonlinear partial differential equations. The expression of pressure rise is evaluated numerically by numerical integration, a built-in technique in mathematical software Mathematica. After discussing the effects of emerging parameters from above graphical investigation, we have achieved the following main conclusions of the study.

1. It is observed that temperature profile is an increasing function of N_b but decreases with β and N_t.
2. Nano particles concentration increases with β and N_b while decreases with N_t.
3. From above analysis, it is measured that the peristaltic pumping rate is varying directly with α , N_b and ϕ but inversely with N_t, B_r and G_r.
4. It is evaluated that pressure gradient profile rises up with α , Q and N_b but declined with B_r, G_r and N_t.
5. Trapping boluses increase in number with G_r and N_b but reduce with increasing α .

References

Akbar NS, Nadeem S (2012) Peristaltic flow of a Phan-Thien-Tanner nanofluid in a diverging tube. Heat Trans Asian Res 41:10–22

Ellahi R, Zeeshan A (2011) A study of pressure distribution for a slider bearing lubricated with a second-grade fluid. Numer Meth Part Diff Eqs 27:1231–1241

Ellahi R, Zeeshan A, Wafai K, Rahman HU (2011) Series solutions for magnetohydrodynamic flow of non-Newtonian nanofluid and heat transfer in coaxial porous cylinder with slip conditions. J Nanoengng Nanosys 225:123–132

He JH (2010) A note on the homotopy perturbation method. Therm Sci 14:565–568

He JH (2006) Homotopy perturbation method for solving boundary value problems. Phys Lett A 350:87-88

Kothandapani M, Srinivas S (2008) Peristaltic transport of a Jeffrey fluid under the effect of magnetic field in an asymmetric channel. Int J Non-Linear Mech 43:915–924

Mekheimer KS, Abdelmaboud Y (2008) Peristaltic flow of a couple stress fluid in an annulus: application of an endoscope. Phys A 387:2403–2415

Mekheimer KhS, Husseny SZ, Abdellateef AI (2011) Effect of lateral walls on peristaltic flow through an asymmetric rectangular duct. Appl Bion Biomech 8:295–308

Mekheimer KS, Abdelmaboud Y, Abdellateef AI (2013) Peristaltic transport through an eccentric cylinders: mathematical model. Appl Bionics Biomech 10:19–27

Nadeem S, Maraj EN (2012) The mathematical analysis for peristaltic flow of nanofluid in a curved channel with compliant walls. Appl Nanosci. doi:10.1007/s13204-012-0165-x

Nadeem S, Riaz A, Ellahi R, Akbar NS (2013) Effects of heat and mass transfer on peristaltic flow of a nanofluid between eccentric cylinders. Appl Nanosci. doi:10.1007/s13204-013-0225-x

Nadeem S, Riaz A, Ellahi R, Akbar NS (2013) Mathematical model for the peristaltic flow of Jeffrey fluid with nano particles phenomenon through a rectangular duct. Appl. Nanosci. doi: 10.1007/s13204-013-0238-5

Patel M, Timol MG (2010) The stress-strain relationship for visco-inelastic non-Newtonian fluids. Int J Appl Math Mech 6:79–93

Rafiq A, Malik MY, Abbasi T (2010) Solution of nonlinear pull-in behavior in electrostatic micro-actuators by using He's homotopy perturbation method. Comput Math Appl 59:2723–2733

Reddy MVS, Mishra M, Sreenadh S, Rao AR (2005) Influence of lateral walls on peristaltic flow in a rectangular duct. J Fluids Eng 127:824–827

Saadatmandi A, Dehghan M, Eftekhari A (2009) Application of He's homotopy perturbation method for non-linear system of second-order boundary value problems. Nonlinear Anal Real World Appl 10:1912–1922

Tripathi D (2011) A mathematical model for the peristaltic flow of chyme movement in small intestine. Math Biosci 233:90–97

Tripathi D, Pandey SK, Das S (2010) Peristaltic flow of viscoelastic fluid with fractional Maxwell model through a channel. Appl Math Comput 215:3645–3654